ACS SENSORS

Article

Cite This: ACS Sens. 2017, 2, 1435-1440

pubs.acs.org/acssensors

Individual Au-Nanocube Based Plasmonic Nanoprobe for Cancer Relevant MicroRNA Biomarker Detection

Lei Zhang,[†] Jinghui Wang,[†] Junxia Zhang,[†] Yuqi Liu,[†] Lingzhi Wu,*[,‡] Jingjing Shen,[†] Ying Zhang,[†] Yanling Hu,[†] Quli Fan,[†] Wei Huang,[†,§] and Lianhui Wang*[,†]

[†]Key Laboratory for Organic Electronics and Information Displays & Institute of Advanced Materials (IAM), National Synergistic Innovation Center for Advanced Materials (SICAM) and [‡]College of Geographic and Biologic Information, Nanjing University of Posts & Telecommunications, 9 Wenyuan Road, Nanjing 210023, China

[§]Key Laboratory of Flexible Electronics (KLOFE) & Institute of Advanced Materials (IAM), National Synergistic Innovation Center for Advanced Materials (SICAM), Nanjing Tech University (Nanjing Tech), 30 South Puzhu Road, Nanjing 211816, China

Supporting Information

ABSTRACT: MicroRNA205 (miR-205), as a significant tumor biomarker, is of vital importance for diagnosis of lung cancer and its overexpression patterns have been extensively studied. Here, we report a novel and label-free nanoprobe with high sensitivity and selectivity for miRNA biomarker detection using localized surface plasmon resonance (LSPR) technology on a single DNA modified gold nanocube (AuNC). This method allowed real-time monitoring of the subtle LSPR scattering peak position's change which was aroused by the variation of dielectric constant in the hybridization process of target miRNA with ssDNA modified on the surface of AuNCs. Notably, the limit of detection of the AuNC-ssDNA probe is up to 5 pM in serum sample, and these results showed that the square structure has more superior sensitivity for design and development of nanoprobe for trace lung cancer relevant miRNAs detection. The better sensing ability and stability of LSPR probe on a AuNC provide potential application to developing a high flux biochip in the future.

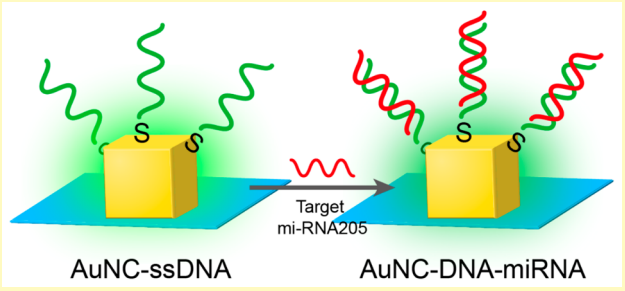

KEYWORDS: *gold nanocubes, microRNA, localized surface plasmon resonance, biosensor, biomarker*

Recently, analysis of cancer biomarkers, such as proteins, DNA, or RNA, has been considered an accurate and effective method in cancer diagnosis. Among all the biomarkers, MicroRNAs (miRNAs), working as protein translation regulators, have especially unique characteristics that enable their use as biomarkers for historical classification, cancer diagnosis, and prognosis.[1] MicroRNA205 (miR-205) has confirmed overexpression in serum and sputa of lung cancer patients. For example, the relative expressions of miR-205 in nonsmall cell lung carcinoma (NSCLC) tissues were upregulated more than 10-fold compared with their expression in cancer adjacent normal tissues (expression levels: miR-205 = 12 356 ± 8741; miR-21 = 674 ± 46).[2] The miR-205 expression levels in NSCLC samples showed a high sensitivity and specificity for diagnosis of NSCLC.[3] Over the past decades, a variety of analytical methods have been used to detect oligonucleotides. Compared with the traditional polymerase chain reaction (PCR) method, a nanoparticle based DNA detecting method has more advantages in accurate localization, visible process, and multiple detection including the colorimetric method,[4] fluorescence method,[5] quantum dot based DNA sensor,[6] surface-enhanced Raman spectroscopy (SERS), and electrochemical method.[7,8] However, it is very hard to distinguish tiny color changes by naked eyes; probes with fluorescence suffer from rapid bleaching and are not bright enough for some applications; toxicity of quantum dot limits its wide use; SERS and electrochemical method can hardly be applied to the analysis of the microsignal, which results in low repeatability. So, SPR signal based measurement at the single nanoparticle level is becoming an effective and ultrasensitive way of oligonucleotide detection due to its positional accuracy, nontoxicity, and real-time monitoring.

Surface plasmon resonance (SPR) scattering signals of noble metal nanoparticles, especially gold (Au) and silver (Ag), possess unique and tunable optical properties.[9,10] These properties contribute to promising research on surface plasmon photonics including surface electric field enhancement, surface enhancement Raman, surface plasmonic photocatalysis, surface energy transfer enhancement, and so on.[11] Besides, the tunable photophysical properties of noble metal nanocrystals and the efficient addressability through optical and spectroscopic techniques make this nanotechnology useful not only in photonics but also in biomedical applications including cell

Received: May 14, 2017
Accepted: August 25, 2017
Published: August 25, 2017

DOI: 10.1021/acssensors.7b00322
ACS Sens. 2017, 2, 1435−1440

Scheme 1. Biosensing Scheme of AuNC-ssDNA Probe Based on the Refelective Index Increase Induced by Hybridization on a Single AuNC Surface

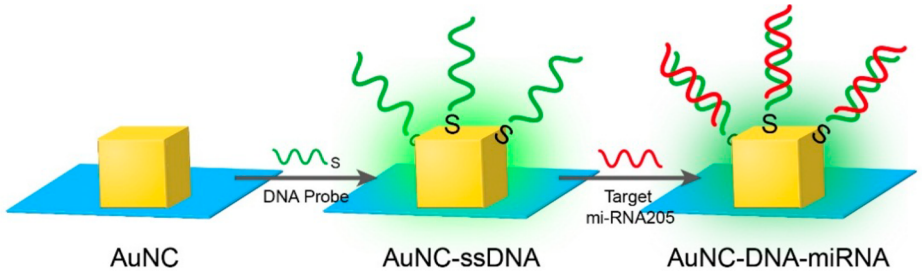

imaging, photothermal therapy, and surface plasmon resonance biosensing.[12−17] Among all the plasmonic research and applications, the surface plasmon resonance biosensor has become one of the most important plasmonic branches. When it is hybridized with target molecules, a notable change of reflective index can be captured,[18] which results in the sensitive detection of target molecules. Compared to normal thin film SPR sensor, a single plasmonic nanoparticle sensor is more sensitive due to its superior application in transmembrane movement,[19] intercell detection,[20] and targeted photodiagnostics and therapy.[21] The effective approach for measuring the surface plasmon scattering light is based on a spectrograph analytical technique of dark-field microscopy (DFM), which can be applied to real-time biosensing of trace biomolecules with high sensitivity and selectivity.[22] For example, the microscopy system assembled by Yi-Tao Long's group has been successfully used with high sensitivity and selectivity to monitor chemistry reactions, electron-transfer processes, cell imaging, and cancer diagnosis.[23−25] Especially, the LSPR scattering biosensor could even distinguish the different structure on a single Ag@Au nanocube surface in our previous report.[26] Therefore, this method provides an alternative method for the detection of trace biomolecular analyses. From the results reported, it was confirmed that the surface plasmon response of nanoparticles was influenced by particles' shapes. The polyhedral nanoparticles with fewer faces and more vertices, such as nanocubes and nanostars, showed stronger surface plasmon resonance effects than nanospheres in a wider energy range.[27]

In this case, we explored an individual gold nanocube based plasmonic nanoprobe modified with thiolated single strand DNA (ssDNA) for the ultrasensitive detection of trace lung cancer marker miR-205. As shown in Scheme 1, when the AuNC-ssDNA probe was hybridized with target oligonucleotides, it will result in a tiny change of dielectric constant of the AuNC surface microenvironment. Hybridization processes with a continue red shift in LSPR scattering spectra can be real-time monitored by the LSPR scattering spectroscopy on an individual nanoparticle. The detection range of this single AuNC-ssDNA probe is from 10 pM to 1 μM with a low limit of detection (LOD) of 5 pM, which is 3 orders of magnitude lower than the nanosphere's, showing its superior detecting sensitivity.[28] The results will provide potential applications in design of plasmonic biochips with sensing cells in nanoscale for high flux analysis of biomarker.

RESULTS AND DISCUSSION

In order to analyze the typical features of AuNCs, some characterization data (UV, TEM, SEM) of the gold nanocubes had been accurately obtained. The UV−vis spectra collected from the AuNCs colloid are shown in Figure 1B. Its maximum peak position was located at 538 nm which is close to the absorption spectrum of ~50-nm-diameter nanosphere but slightly red-shifted.[29] The size, yield, and structure of AuNCs were further characterized using TEM. From the TEM images, we can determine that the length of the AuNC is around 50 nm and the vertices are slightly rounded and the yield is about 80% by general counting. As we know, the size of the gold nanoparticles (AuNPs) has a vital influence on the LSPR signal intensity of noble metal nanoparticles.[30]

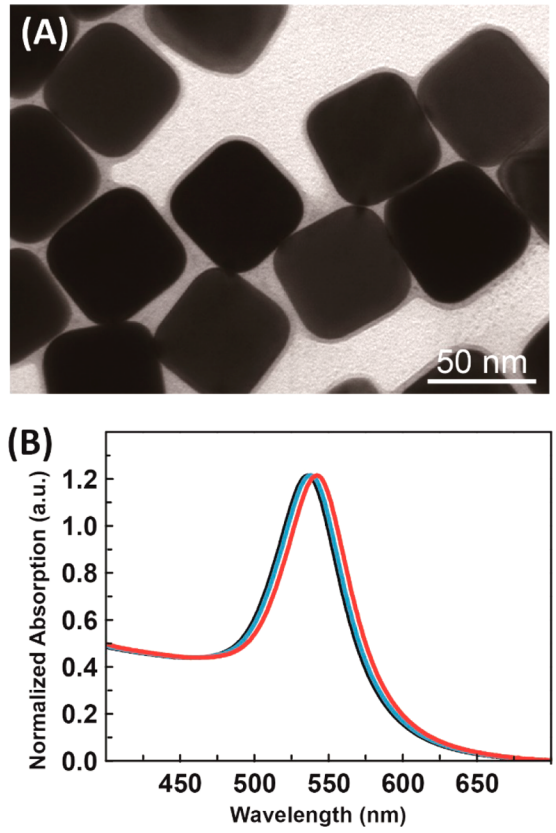

Figure 1. (A) TEM image of ~50 nm AuNCs. (B) Normalized UV−vis absorption spectra of colloidal AuNCs (black), AuNCs-ssDNA (blue), and AuNCs-ssDNA in 100 μM miR-205 solution (red).

Smaller AuNPs (diameter < 40 nm) presented dull green light for which scattering spectra are difficult for capture, while larger sized AuNPs present green or even red color that enable a much more sensitive signal under the DFM. It obviously applies the same to our cubical nanoparticles and that is why AuNCs with edge length over 40 nm were chosen.[31,32] During

DOI: 10.1021/acssensors.7b00322
ACS Sens. 2017, 2, 1435−1440

the synthesis process, Au nanocubes with different edge lengths were attempted by changing the reagents' dosage, but larger-sized particle morphology was hard to control, which results in a decrease in the particle yield. By repeated experiments, the morphology and yield of Au nanocubes with 50 nm edge length can be controlled best.

However, getting the accurate SPR spectrum signal of the AuNC needs further confirmation of morphology and color under a dark field microscope (DFM), which results in characterization of in situ SEM images. Individual AuNC immobilized on the substrate glass slide could be observed through color photographs obtained by color CCD of DFM. ImageJ software was used to measure the distance between the mark and the single AuNC whose shape was supposed to be a 50 nm edge length nanocube, and then the in situ SEM protocol was employed to obtain the real condition of the specific AuNC on ITO glass slide. Figure 2A showed the DFM image of the nanocubes. The in situ SEM image (Figure 2B) helps to confirm that those dark green points are the right AuNC-particles. Besides, the comparison of AuNC morphology before and after hybridization can also be obtained by in situ SEM characterization. SEM images of AuNC based probe were given to exhibit its shape and size clearly before (Figure 2B left) and after (Figure 2B right) hybridization with target miRNAs, and there was no distinct change in AuNC shape when the probe ssDNA hybridized with target miRNA. Therefore, due to its high synthesis yield and easy shape control, ~50 nm AuNCs could be chosen to fabricate LSPR nanobiosensors. As a comparison, the UV−vis spectra of AuNCs-ssDNA solution and the probe solutions with 10 μM miR-205 were shown in Figure 1B and Figure S1, respectively. These results could simply prove that hybridization occurred on the AuNCs surface but with lower S/N ratio.

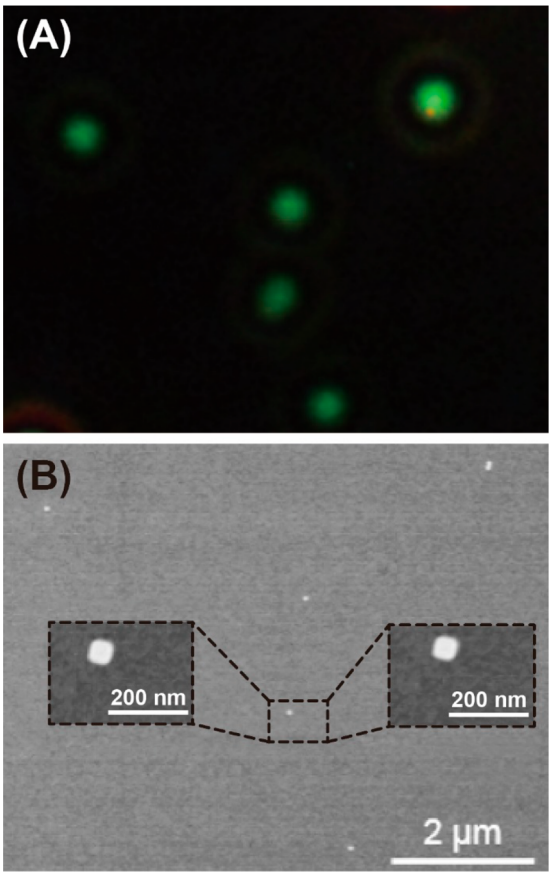

Figure 2. (A) Dark-field image of AuNC-ssDNA before hybridization with miRNA on ITO. (B) In situ SEM images of AuNC-ssDNA in the selected area of (A); the inset images were the detailed view of one selected AuNC-ssDNA before (left) and after (right) hybridization with miR-205.

Individual AuNC modified with thiolated ssDNA molecule could be used for target RNA detection through hybridization reaction which results in a tiny change of the reflective index of the surface microenvironment, and then there would be a certain red-shift in their LSPR scattering spectra (Figure S3). To determine the sensitivity of the probe, the concentration and the modification time of ssDNA connected with the AuNCs must be decided. The concentration of the AuNC aqueous solution used to soak the ITO slide is about 1 nM, so that we choose 1 μM of ssDNA to modify our AuNCs, which can ensure the full-scale modification of our particles. Besides, various modification times of ssDNA on the AuNCs surface was carried out in analytical experiments with 1 μM target miRNA, and we could observe that the peak shift of LSPR scattering spectra of a single nanoparticle achieved the max value and then slightly decreased after 2 h, which indicated that long-term modification inducing an overload of probe ssDNA could prevent the target oligonucleotides from hybridizing[33] (Figure 3D). For all of the above, 2 h modification time of probe ssDNA was applied in the follow-up experiments with concentration of 1 μM.

Target RNA solution was added onto the AuNC-ssDNA sensing chip, and then the LSPR scattering spectra of individual AuNC were continuously captured over 2 h. After the hybridization, the initial scattering peaks of these AuNC-ssDNA probes located around 560 nm were red-shifted to longer wavelength (Figure 3A). The degree of red-shifting of the LSPR scattering spectrum peak is dependent on the target molecule concentration, indicating an increase in the reflective index near Au due to the higher refractive index of double strand nucleic acid than ssDNA.[34] Figure 3B was the corresponding plot of single AuNC-ssDNA's LSPR scattering spectra shift, which was dependent on time; the peak shift range of the LSPR scattering spectra of single AuNC-ssDNA increased rapidly at the beginning stage and reached a limit versus different concentrations (10 pM, 100 pM, 1 nM, 10 nM, 100 nM, 1 μM) of target miRNA with a shift from 0.9 to 5 nm. The results proved that the red-shift in scattering spectra was mainly caused by hybridization of probe ssDNA and target miR-205 on a selected individual AuNC surface. As shown in Figure 3C, a linear relationship ($\Delta\lambda = 0.74 \times \log_{10} C_{miR} + 2.33$) between the peak shift and the miR-205 concentration was observed. The peak shift value decreased to 0.9 nm within the margin of error with the concentration limited to 10 pM. The successful analysis of miR-205 by the LSPR scattering spectra peak shift exhibited higher sensitivity than some previously reported results on an individual nanoparticle.[28]

Single AuNC based biosensors have proven useful for the label-free detection of miRNAs. In our research, miR-205 was chosen as target miRNA due to its overexpression in lung cancers.[35] In particular, it could be regarded as a useful biomarker in the early detection of nonsmall cell lung cancer (NSCLC) accounts for over 80% of all lung cancer cases worldwide.[36] However, to ensure the accuracy and sensitivity of the detection, contrast experiments are necessary. Three RNAs with different sequences were chosen to be involved in contrast

DOI: 10.1021/acssensors.7b00322
ACS Sens. 2017, 2, 1435−1440

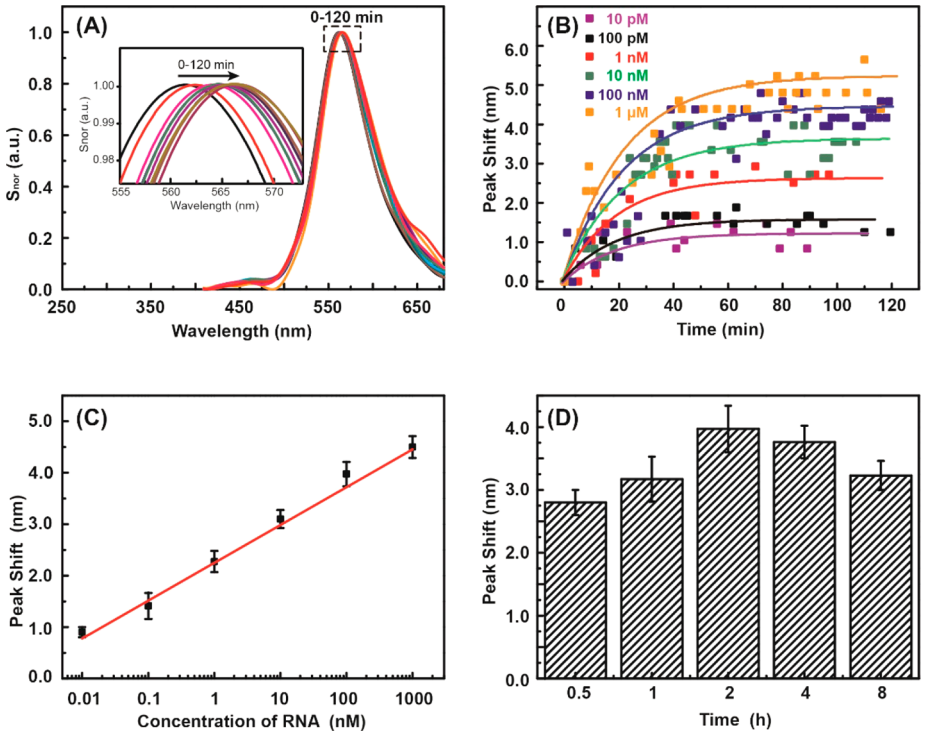

Figure 3. (A) LSPR scattering spectra of one AuNC-ssDNA probe treated with 1 μM miRNA sample at different times. (B) LSPR spectra peak red-shifts with the time on various AuNC-ssDNA probes with miR-205 in different concentrations (10 pM, 100 pM, 1 nM, 10 nM, 100 nM, 1 μM). (C) Calibration curve of the LSPR peak shift versus different concentrations of miR-205 (10 pM, 100 pM, 1 nM, 10 nM, 100 nM, 1 μM). (D) LSPR Peak shift after treatment of 100 nM target miR-205 with different modification times of 1 μM probe ssDNA.

and hybridization with the AuNC-ssDNA probes, including miR-205, single-mismatch miR-205, and random RNA. LSPR scattering spectra were recorded during the sensing experiments. All the detection experiments were done in ultrapure water buffer solution. As shown in Figure 4A, when the hybridization was performed with the same concentration of 100 nM sample, the result was about 4.5 nm red-shift between ssDNA and miR-205, and there was a scarce LSPR peak shift when the AuNC-ssDNA probes were placed in random RNA solution, but the peak position change in the LSPR spectra of single-base mismatch mi-RNA notably decreased to 1.5 nm. The results suggested that the AuNC-ssDNA nanosensor could be used for discriminating target miRNA from other interference biomolecules with high selectivity. However, practical use requires further research on the sensing ability of the AuNC-ssDNA probe based on this plasmonic nanobiosensor in fetal bovine serum (FBS). In a 50× diluted FBS without miR-205, which acted as a control, there was almost no red-shift in the LSPR peak position. Then a sequence of sensing experiments with different miR-205 concentrations were performed in 2% FBS. With the presence of miR-205 whose concentration increased from 10 pM to 1 μM, the red-shift degree of LSPR scattering spectra also increased proportionally, which is similar to miR-205 in aqueous solution (Figure 4B). The LSPR spectra red-shift exhibited good linearity with the concentration of miR-205 in a wide range with a low LOD up to 5 pM in serum sample (the LOD was caculated when S/N was 3). The results provided an alternative method with more sensitivity for the real sample analysis.[28]

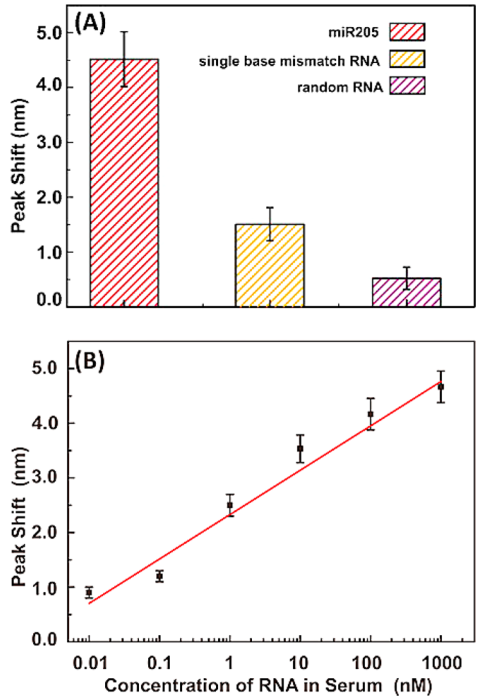

Figure 4. (A) Peak shift of AuNCs-ssDNA probes' scattering spectra under different interference conditions: 1, miR205 for control (100 nM, red); 2, single base mismatch miRNA (100 nM, orange); 3, random miRNA (100 nM, purple). (B) Calibration curve of the LSPR scattering spectra peak shift with treatment of different concentrations of miR-205 (10 pM, 100 pM, 1 nM, 10 nM, 100 nM, 1 μM) in the serum.

DOI: 10.1021/acssensors.7b00322
ACS Sens. 2017, 2, 1435−1440

CONCLUSION

We developed a simple and effective AuNC-ssDNA based SPR nanoprobe for label-free detection of miR-205, a typical biomarker of lung cancer, at single nanoparticle level. As the hybridization happened between the AuNCs-ssDNA SPR probe and the target miRNA, the peak of the SPR spectra would shift to a longer wavelength. The LSPR spectral red shift depending on time displays a good linearity in a wide range with a low LOD up to 5 pM in serum sample. The accurate discrimination among original, single base mismatched and random RNA manifest the high sensitivity and excellent selectivity of this LSPR probe in the serum sample. Comparison with the detection efficiency between Au-nanosphere, Au-nanocube probe agrees with theoretical analysis about the influence of the nanocrystal configuration, which demonstrates that more vertexes induce more surface plasmons in a wider energy range. The successful application of the single AuNCs-ssDNA SPR probe can be used as an effective and sensitive method for the trace cancer biomarker detection and can potentially be used in designing a high flux analysis biochip for early diagnostics of lung cancer in the future.

ASSOCIATED CONTENT

Supporting Information

The Supporting Information is available free of charge on the ACS Publications website at DOI: 10.1021/acssensors.7b00322.

UV−vis spectra of AuNCs plasmonic probe; peak shift of the UV−vis spectra; original LSPR scattering spectra (PDF)

AUTHOR INFORMATION

Corresponding Authors

*E-mail: wulz@njupt.edu.cn.
*E-mail: iamlhwang@njupt.edu.cn.

ORCID

Lingzhi Wu: 0000-0002-0045-2539
Quli Fan: 0000-0002-9387-0165
Lianhui Wang: 0000-0001-9030-9172

Author Contributions

All authors have given approval to the final version of the manuscript.

Notes

The authors declare no competing financial interest.

ACKNOWLEDGMENTS

This work was supported by the National Natural Science Foundation of China (21475064, 61571239, 21674048, 61705113), Sci-tech Support Plan of Jiangsu Proince (BE2014719), the Program for Changjiang Scholars and Innovative Research Team in University (IRT_15R37), the Scientific Research Foundation of Nanjing University of Posts and Telecommunications (NY215173), and the Priority Academic Program Development of Jiangsu Higher Education Institutions (17KJB416008, YX03001, NY217007).

REFERENCES

(1) Montani, F.; Marzi, M. J.; Dezi, F.; Dama, E.; Carletti, R. M.; Bonizzi, G.; Bertolotti, R.; Bellomi, M.; Rampinelli, C.; Maisonneuve, P.; et al. miR-Test: a blood test for lung cancer early detection. *J. Natl. Cancer Inst.* **2015**, *107*, djv063.

(2) Jiang, M.; Zhang, P.; Hu, G.; Xiao, Z.; Xu, F.; Zhong, T.; Huang, F.; Kuang, H.; Zhang, W. Relative expressions of miR-205−5p, miR-205−3p, and miR-21 in tissues and serum of non-small cell lung cancer patients. *Mol. Cell. Biochem.* **2013**, *383*, 67−75.

(3) Lebanony, D.; Benjamin, H.; Gilad, S.; Ezagouri, M.; Dov, A.; Ashkenazi, K.; Gefen, N.; Izraeli, S.; Rechavi, G.; Pass, H.; Nonaka, D.; Li, J.; Spector, Y.; Rosenfeld, N.; Chajut, A.; Cohen, D.; Aharonov, R.; Mansukhani, M. Diagnostic assay based on hsa-miR-205 expression distinguishes squamous from nonsquamous non-small-cell lung carcinoma. *J. Clin. Oncol.* **2009**, *27*, 2030−2037.

(4) Zhou, Z.; Wei, W.; Zhang, Y.; Liu, S. DNA-responsive disassembly of AuNP aggregates: influence of nonbase-paired regions and colorimetric DNA detection by exonuclease III aided amplification. *J. Mater. Chem. B* **2013**, *1*, 2851−2858.

(5) Liu, S.; Wang, L.; Luo, Y.; Tian, J.; Li, H.; Sun, X. Polyaniline nanofibres for fluorescent nucleic acid detection. *Nanoscale* **2011**, *3*, 967−969.

(6) Chen, B.; Meinertzhagen, I.; Shaw, S. Circadian rhythms in light-evoked responses of the fly's compound eye, and the effects of neuromodulators 5-HT and the peptide PDF. *J. Comp. Physiol., A* **1999**, *185*, 393−404.

(7) Braun, G.; Lee, S. J.; Dante, M.; Nguyen, T.-Q.; Moskovits, M.; Reich, N. Surface-enhanced Raman spectroscopy for DNA detection by nanoparticle assembly onto smooth metal films. *J. Am. Chem. Soc.* **2007**, *129*, 6378−6379.

(8) Drummond, T. G.; Hill, M. G.; Barton, J. K. Electrochemical DNA sensors. *Nat. Biotechnol.* **2003**, *21*, 1192−1199.

(9) Biswas, P.; Cho, S. R.; Kim, J. W.; Baek, S. D.; Myoung, J. M. Improved UV response of ZnO nanotubes by resonant coupling of anchored plasmonic silver nanoparticles. *Nanotechnology* **2017**, *28*, 225502.

(10) Jain, P. K.; Huang, X.; El-Sayed, I. H.; El-Sayed, M. A. Review of some interesting surface plasmon resonance-enhanced properties of noble metal nanoparticles and their applications to biosystems. *Plasmonics* **2007**, *2*, 107−118.

(11) Ozbay, E. Plasmonics: merging photonics and electronics at nanoscale dimensions. *Science* **2006**, *311*, 189−193.

(12) Zhu, Z.; Zou, Y.; Hu, W.; Li, Y.; Gu, Y.; Cao, B.; Guo, N.; Wang, L.; Song, J.; Zhang, S.; Gu, H.; Zeng, H. Near-Infrared Plasmonic 2D Semimetals for Applications in Communication and Biology. *Adv. Funct. Mater.* **2016**, *26*, 1793−1802.

(13) Huang, X.; El-Sayed, I. H.; Qian, W.; El-Sayed, M. A. Cancer cell imaging and photothermal therapy in the near-infrared region by using gold nanorods. *J. Am. Chem. Soc.* **2006**, *128*, 2115−2120.

(14) Fong, K. E.; Yung, L.-Y. L. Localized surface plasmon resonance: a unique property of plasmonic nanoparticles for nucleic acid detection. *Nanoscale* **2013**, *5*, 12043−12071.

(15) Thakur, A.; Qiu, G.; Ng, S.-P.; Guan, J.; Yue, J.; Lee, Y.; Wu, C.-M. L. Direct detection of two different tumor-derived extracellular vesicles by SAM-AuNIs LSPR biosensor. *Biosens. Bioelectron.* **2017**, *94*, 400−407.

(16) Zhang, Y.; Zhu, C.; Zhang, L.; Tan, C.; Yang, J.; Chen, B.; Wang, L.; Zhang, H. DNA-templated silver nanoclusters for multiplexed fluorescent DNA detection. *Small* **2015**, *11*, 1385−1389.

(17) Wang, Z.; Zhang, J.; Zhu, C.; Wu, S.; Mandler, D.; Marks, R. S.; Zhang, H. Amplified detection of femtomolar DNA based on a one-to-few recognition reaction between DNA-Au conjugate and target DNA. *Nanoscale* **2014**, *6*, 3110−3115.

(18) Zhu, J.; Li, J.-j.; Zhao, J. -w., Optimizing the plasmonic sensing of RNA folding based on local refractive index change of gold nanorod. *Appl. Surf. Sci.* **2013**, *275*, 264−268.

(19) Papo, N.; Shai, Y. Exploring peptide membrane interaction using surface plasmon resonance: differentiation between pore formation versus membrane disruption by lytic peptides. *Biochemistry* **2003**, *42*, 458−466.

(20) Ankri, R.; Meiri, A.; Lau, S. I.; Motiei, M.; Popovtzer, R.; Fixler, D. Intercoupling surface plasmon resonance and diffusion reflection measurements for real-time cancer detection. *J. Biophotonics* **2013**, *6*, 188−196.

DOI: 10.1021/acssensors.7b00322
ACS Sens. 2017, 2, 1435−1440

(21) Jain, P. K.; El-Sayed, I. H.; El-Sayed, M. A. Au nanoparticles target cancer. *Nano Today* **2007**, *2*, 18−29.
(22) Long, Y.-T.; Jing, C. *Localized Surface Plasmon Resonance Based Nanobiosensors*; Springer, 2014.
(23) Shi, L.; Jing, C.; Ma, W.; Li, D. W.; Halls, J. E.; Marken, F.; Long, Y. T. Plasmon Resonance Scattering Spectroscopy at the Single-Nanoparticle Level: Real-Time Monitoring of a Click Reaction. *Angew. Chem., Int. Ed.* **2013**, *52*, 6011−6014.
(24) Zhang, L.; Li, Y.; Li, D. W.; Jing, C.; Chen, X.; Lv, M.; Huang, Q.; Long, Y. T.; Willner, I. Single Gold Nanoparticles as Real-Time Optical Probes for the Detection of NADH-Dependent Intracellular Metabolic Enzymatic Pathways. *Angew. Chem., Int. Ed.* **2011**, *50*, 6789−6792.
(25) Ma, W.; Ying, Y.-L.; Qin, L.-X.; Gu, Z.; Zhou, H.; Li, D.-W.; Sutherland, T. C.; Chen, H.-Y.; Long, Y.-T. Investigating electron-transfer processes using a biomimetic hybrid bilayer membrane system. *Nat. Protoc.* **2013**, *8*, 439−450.
(26) Tian, Y.; Zhang, L.; Shen, J.; Wu, L.; He, H.; Ma, D.-L.; Leung, C.-H.; Wu, W.; Fan, Q.; Huang, W.; Wang, L. An Individual Nanocube-Based Plasmonic Biosensor for Real-Time Monitoring the Structural Switch of the Telomeric G-Quadruplex. *Small* **2016**, *12*, 2913−2920.
(27) Noguez, C. Surface plasmons on metal nanoparticles: the influence of shape and physical environment. *J. Phys. Chem. C* **2007**, *111*, 3806−3819.
(28) Hu, Y.; Zhang, L.; Zhang, Y.; Wang, B.; Wang, Y.; Fan, Q.; Huang, W.; Wang, L. Plasmonic nanobiosensor based on hairpin DNA for detection of trace oligonucleotides biomarker in cancers. *ACS Appl. Mater. Interfaces* **2015**, *7*, 2459−2466.
(29) Kou, X.; Sun, Z.; Yang, Z.; Chen, H.; Wang, J. Curvature-directed assembly of gold nanocubes, nanobranches, and nanospheres. *Langmuir* **2009**, *25*, 1692−1698.
(30) Link, S.; El-Sayed, M. A. Size and temperature dependence of the plasmon absorption of colloidal gold nanoparticles. *J. Phys. Chem. B* **1999**, *103*, 4212−4217.
(31) Haiss, W.; Thanh, N. T.; Aveyard, J.; Fernig, D. G. Determination of size and concentration of gold nanoparticles from UV− Vis spectra. *Anal. Chem.* **2007**, *79*, 4215−4221.
(32) Truong, P. L.; Ma, X.; Sim, S. J. Resonant Rayleigh light scattering of single Au nanoparticles with different sizes and shapes. *Nanoscale* **2014**, *6*, 2307−2315.
(33) Steel, A. B.; Herne, T. M.; Tarlov, M. J. Electrochemical quantitation of DNA immobilized on gold. *Anal. Chem.* **1998**, *70*, 4670−4677.
(34) Zhang, L.; Zhang, Y.; Hu, Y.; Fan, Q.; Yang, W.; Li, A.; Li, S.; Huang, W.; Wang, L. Refractive index dependent real-time plasmonic nanoprobes on a single silver nanocube for ultrasensitive detection of the lung cancer-associated miRNAs. *Chem. Commun.* **2015**, *51*, 294−297.
(35) Baffa, R.; Fassan, M.; Volinia, S.; O'Hara, B.; Liu, C. G.; Palazzo, J. P.; Gardiman, M.; Rugge, M.; Gomella, L. G.; Croce, C. M.; et al. MicroRNA expression profiling of human metastatic cancers identifies cancer gene targets. *J. Pathol.* **2009**, *219*, 214−221.
(36) Markou, A.; Tsaroucha, E. G.; Kaklamanis, L.; Fotinou, M.; Georgoulias, V.; Lianidou, E. S. Prognostic value of mature microRNA-21 and microRNA-205 overexpression in non-small cell lung cancer by quantitative real-time RT-PCR. *Clin. Chem.* **2008**, *54*, 1696−1704.

DOI: 10.1021/acssensors.7b00322
ACS Sens. 2017, 2, 1435−1440